only random variations in intensity during data collection.

Calculations were performed as described above on data that had been corrected for Lorentz and polarization effects. Iridium and gold heavy atom positions were determined via Patterson methods. All non-carbon atoms of the cation along with the carbonyl carbon, C(1), were refined with anisotropic thermal parameters, while all others were refined with isotropic thermal parameters. All phenyl rings were modeled as rigid groups. Bond lengths and angles were also fixed for the hexafluorophosphate ion. The hydrogen atom positions on methylene carbons were included by using a riding model with a C–H vector fixed at 0.96 Å and a thermal parameter 1.2 times the host carbon. An absorption correction was applied.[22] The largest peak in the final difference map had density equal to 7.0 electrons/Å^3. This peak is 0.991 Å from Au(1).

$[Ir(CN)_2Au_2(\mu\text{-dpmp})_2][PF_6]$. Dichroic purple/gold crystals were obtained with difficulty by slow diffusion of toluene into a dichloromethane solution of the complex. The crystal was handled as described above. Unit cell parameters were determined by least-squares refinement of 11 reflections with $16 < 2\theta < 23°$. Two check reflections exhibited only random (<2%) variation during data collection. Crystal data are given in Table IV.

Calculations were performed as previously outlined. Iridium and gold heavy atom positions were determined from a Patterson map with the iridium positioned on the inversion center. All non-carbon atoms of the cation along with the cyanide carbon, C(1), were refined with anisotropic thermal parameters, while all others were refined with isotropic thermal parameters. The hydrogen atom positions were calculated by using a riding model with a C–H vector fixed at 0.096 Å and a thermal parameter 1.2 times the host carbon. An absorption correction was applied.[28]

There are two toluene molecules in the crystal lattice. One of these is disordered. For the latter, atomic positions are shared for six phenyl carbon atoms, while the methyl group is disordered between two para positions. A dichloromethane molecule is also present in the lattice at 25% occupancy. The largest unassigned peak in the final difference map had density equal to 8.3 electrons/Å^3. This peak is 0.571 Å from Ir(1). A 3 electrons/Å^3 peak is located at (0.5, 0.5, 0) but represents an unreasonable contact with the PF_6^- anion. The goodness of fit was calculated at 1.477.

Acknowledgment. We thank the National Science Foundation (Grant CHE 894209) for support, Johnson Matthey, Inc. for a loan of gold and iridium salts, and Professor Peter B. Kelly for experimental assistance.

Supplementary Material Available: Tables of atomic coordinates, bond distances, angles, anisotropic thermal parameters, hydrogen atom positions, and refinement data for **4**, **6**, and **7** (22 pages); tables of observed and calculated structure factors (102 pages). Ordering information is given on any current masthead page.

Reactions of Aryl–Iron(III) Porphyrins with Dioxygen. Formation of Aryloxy–Iron(III) and Aryl–Iron(IV) Complexes

Ramesh D. Arasasingham,[†] Alan L. Balch,*[,†] Rebecca L. Hart,[†] and Lechosław Latos-Grażyński[‡]

Contribution from the Departments of Chemistry, University of California, Davis, California 95616, and the University of Wrocław, Wrocław, Poland. *Received December 1, 1989*

Abstract: The reaction of dioxygen with low-spin, five-coordinate complexes, $PFe^{III}Ar$ (P, porphyrin dianion; Ar, aryl group) has been examined for comparison with previous work (Arasasingham, R. D. et al. *J. Am. Chem. Soc.* **1989**, *111*, 4357) on the corresponding alkyl complexes which showed that peroxo complexes $PFe^{III}OOR$ formed initially and then decomposed to form PFeOH and an aldehyde or ketone when R was a primary or secondary alkyl group. Dioxygen addition to $TTPFe^{III}(C_6H_4CH_3\text{-}p)$ at 25 °C in toluene yields the phenoxide complex, $TTPFe(OC_6H_4CH_3\text{-}p)$, as the principle product, while addition to $TTPFe^{III}C_6H_5$ at −30 °C yields $TTPFe^{III}OC_6H_5$ and small amounts of $TTPFe^{III}(OC_6H_4OH\text{-}p)$ and $TTPFe^{III}OC_6H_4OFe^{III}TTP$. These reactions have been monitored by both ^1H NMR and ESR spectroscopies. No intermediates have been detected in the formation of these products. Mechanisms for the formation of these products have been formulated in terms of the initial insertion of dioxygen into the Fe–C bond followed by rapid homolysis to form $PFe^{IV}{=}O$ and $^{\bullet}OAr$, with subsequent reactions yielding the final products. Addition of dioxygen to a solution of $TTPFe^{III}(C_6H_4CH_3\text{-}p)$ in chloroform at −60 °C yields a mixture of $[TTPFe^{IV}(C_6H_4CH_3\text{-}p)]^+$ and $TTPFe^{III}Cl$ with no evidence for the formation of the phenoxide complexes. In this case electron transfer to yield the oxidized iron porphyrin and superoxide ion is driven by the solvent polarity and the ability of the solvent to destroy superoxide ion as it is formed.

Introduction

The inactivation of hemoglobin and myoglobin by arylhydrazines in the presence of dioxygen leads to the formation of green pigments which have been identified as *N*-phenylheme.[1-3] Spectroscopic and chemical studies,[3-5] including X-ray structural analysis on the myoglobin complex,[6] have unambiguously demonstrated that phenyl–iron(III) porphyrins are key intermediates in this process. Studies on natural hemeproteins and on model systems have demonstrated that the phenyl group migrates from the iron to the nitrogen under oxidizing conditions.[2-10] Electrochemical and optical spectroscopic studies have suggested that this process occurs via several intermediates as shown in Scheme I.

Scheme I

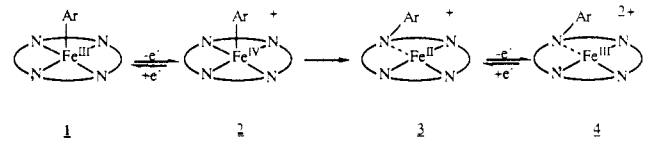

[†] University of California, Davis.

[‡] University of Wrocław.

[§] Abbreviations used: P, porphyrin dianion; TTP, tetra-*p*-tolylporphyrin dianion; TMP, tetramesitylporphyrin dianion; OEP, octaethylporphyrin dianion; Ar, generic aryl group.

(1) Saito, S.; Itano, H. A. *Proc. Natl. Acad. Sci.* U.S.A. **1981**, *78*, 5508.
(2) Ortiz de Montellano, P. R.; Kunze, K. L. *J. Am. Chem. Soc.* **1981**, *103*, 6534.
(3) Augusto, O.; Kunze, K. L.; Ortiz de Montellano, P. R. *J. Biol. Chem.* **1982**, *257*, 6231.
(4) Kunze, K. L.; Ortiz de Montellano, P. R. *J. Am. Chem. Soc.* **1983**, *105*, 1380.

0002-7863/90/1512-7566$02.50/0 © 1990 American Chemical Society

Table I. NMR Resonances for TTPFe^{III}OR Complexes at 25 °C in Toluene-d_8

ligand	ortho	meta	para	pyrr
$C_6H_5O^-$ [a]	−118.4	95.0	−109.7	80.5
p-$CH_3C_6H_4O^-$ [a]	−124.8	97.9	126.9	80.3
m-$CH_3C_6H_4O^-$	−123.4	98.5 (H)	−114.0	80.0
		−37.1 (Me)		
o-$CH_3C_6H_4O^-$	−126.3 (H)	110.9	−120	80
	95.4 (Me)	99.9		
p-$HOC_6H_4O^-$	−130.2	90.9		79.8
o-$HOC_6H_4O^-$	*b*	86.3	−96.4	78.4
		70.2		
o-(o-HOC_6H_4)$C_6H_4O^-$ [a]	−83.6	70.4	−81.8	79.1
		83.6		
p-(C_6H_5O)$C_6H_4O^-$	−124.5	92.1		80.0
p-$CH_3OC_6H_4O^-$	−130.9	91.1	16.3	80.3
(p-CH_3)(o-OCH_3)-$C_6H_3O^-$	−130.1 (H)	75.4	133.7	78.8
	13.2 (OMe)	88.1		

[a] At 22 °C. [b] Not observed presumably because of large line width.

The low-spin ($S = 1/2$), 15-electron PFe^{III}(Ar) complexes have been subject to extensive characterization including ^{1}H NMR spectroscopy[11-15] and X-ray crystallography.[16] Recent ^{1}H NMR studies on the one-electron oxidation of PFe^{III}(Ar) by bromine have shown the formation of the transient phenyl–iron(IV) porphyrin complex that undergoes reductive elimination to produce an iron(II) complex of an N-substituted porphyrin.[10] In protein systems the phenyl migration occurs under aerobic conditions. Our initial observations indicated that dioxygen was also capable of producing one-electron oxidation of PFe^{III}(Ar) to [PFe^{IV}(Ar)]$^+$. Related studies on alkyl–iron(III) complexes revealed a different pattern of reactivity. In toluene solution these react with dioxygen according to reactions 1–3 and yield high-spin ($S = 5/2$), five-coordinate alkyl peroxide complexes of iron(III) as intermediates that can be spectroscopically observed at low temperature (below −70 °C).[17-19] These observations raise the question of whether

$$PFe^{III}CR'R_2 + O_2 \rightarrow PFe^{III}OOCR'R_2 \quad (1)$$

$$PFe^{III}OOCR'R_2 \rightarrow PFe^{III}OH + O{=}CR_2\ (R' = H) \quad (2)$$

$$2PFe^{III}OH \rightarrow PFe^{III}OFe^{III}P \quad (3)$$

similar insertions of dioxygen into the Fe–C bond of the aryl complexes can occur. The report by Ogoshi and co-workers[11] that treating OEPFe^{III}(Ph) with dioxygen in boiling benzene yielded OEPFe^{III}OFe^{III}OEP and bibenzyl as the only reported products further suggested that other pathways for oxidation could occur. Here we describe experiments that demonstrate that the products obtained upon addition of dioxygen to PFe^{III}Ar are very sensitive to reaction conditions and propose explanations for these variations.

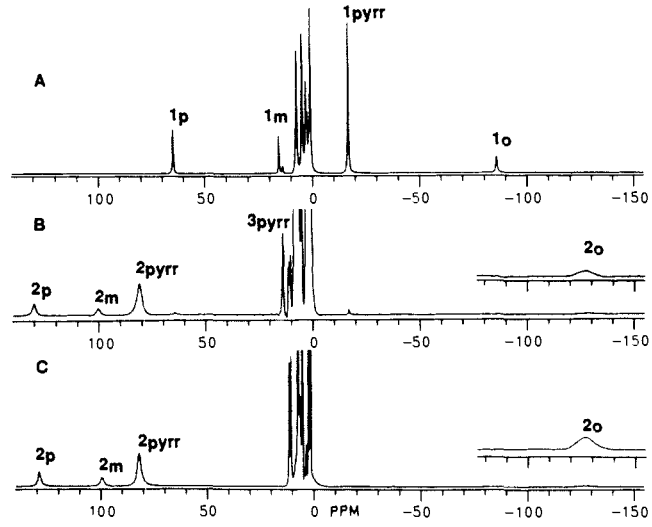

Figure 1. 300-MHz ^{1}H-NMR spectra of toluene-d_8 solutions at 25 °C: (A) TTPFe^{III}($C_6H_4CH_3$-p), (B) TTPFe^{III}($C_6H_4CH_3$-p) after addition of dioxygen, and (C) TTPFe^{III}($OC_6H_4CH_3$-p). Resonances due to TTPFe^{III}($C_6H_4CH_3$-p) are labeled 1, TTPFe^{III}($OC_6H_4CH_3$-p), 2, TTPFe^{III}OFe^{III}TTP, 3. Subscripts identify individual functional groups: pyrr, pyrrole; o, m, ortho, meta protons of the axial p-tolyl or p-cresol ligand; p, p-methyl of the axial p-tolyl or p-cresol ligand.

Results

^{1}H-NMR Characteristics of Phenoxy Complexes. As we shall demonstrate (vide infra) aryloxy complexes, TTPFe^{III}(OAr), can be formed by the reaction of TTPFe^{III}(Ar) with dioxygen. In order to facilitate the identification of aryloxy ligands formed during oxidations, we have obtained the ^{1}H NMR spectra of a number of likely products. These high-spin ($S = 5/2$), five-coordinate aryloxy derivatives were obtained by the reaction of PFe^{III}Cl with the sodium salt of a phenol. The ^{1}H NMR data are collected in Table I. The spectrum of a typical example, TTPFe^{III}($OC_6H_4CH_3$-p), is shown in trace C of Figure 1. Resonance assignments for these ligands are based upon previous assignments of aryloxy complexes of iron(III),[20-23] consideration of the symmetry of the particular aryloxy ligand, intensities of the resonances, and line widths. The data show that there are clear distinctive chemical shift regions for particular functional groups and informative line widths on the axial ligands. At 25 °C the characteristics of these aryloxy ligands are as follows; o-H, −118 to −131 ppm (line width, 2000 Hz), o-CH_3, 95 ppm, m-H, 70–110 ppm (line width 440–500 Hz), m-CH_3, −37 ppm, p-H, −82 to −120 ppm (line width, 400 Hz), p-CH_3, 127–134 ppm. A pyrrole resonance occurs in the 78–81-ppm region with a line width of ca. 550 Hz. As established earlier,[20-23] the alternating shift pattern for H and Me substituents and opposite sign of the shifts for meta versus para or ortho protons are indicative of π spin delocalization on the aryloxy ligands. The line widths of various functional groups reflect the distance of these from the paramagnetic iron center. These data indicate that it should be possible to observe and identify the individual aryloxy complexes if and when they are oxidation products.

Oxygenation of Aryl–Iron(III) Complexes in Toluene Solution. Figure 1 shows the effects of adding dioxygen to a toluene-d_8 solution of TTPFe^{III}($C_6H_4CH_3$-p) at 25 °C. Trace A shows the spectrum of the starting material, while trace B shows the sample following the addition of dioxygen after 25 min. New resonances

(5) Ortiz de Montellano, P. R.; Kerr, D. E. *Biochemistry* **1985**, *24*, 1147.
(6) Ringe, D.; Petsko, G. A.; Kerr, D. E.; Ortiz de Montellano, P. R. *Biochemistry* **1984**, *23*, 2.
(7) Ortiz de Montellano, P. R.; Kunze, K. L.; Augusto, O. *J. Am. Chem. Soc.* **1982**, *104*, 3545.
(8) Mansuy, D.; Battioni, J. P.; Dupre, D.; Sartori, E.; Chottard, G. *J. Am. Chem. Soc.* **1982**, *104*, 6159.
(9) Lancon, D.; Cocolios, P.; Guilard, R.; Kadish, K. M. *J. Am. Chem. Soc.* **1984**, *106*, 4472.
(10) Balch, A. L.; Renner, M. W. *J. Am. Chem. Soc.* **1986**, *108*, 2603.
(11) Ogoshi, H.; Sugimoto, H.; Yoshida, Z.-I.; Kobayashi, H.; Sakai, H.; Maeda, Y. *J. Organomet. Chem.* **1982**, *214*, 185.
(12) Cocolios, P.; Laviron, E.; Guilard, R. *J. Organomet. Chem.* **1982**, *228*, C39.
(13) Cocolios, P.; Lagrange, G.; Guilard, R. *J. Organomet. Chem.* **1983**, *253*, 65.
(14) Balch, A. L.; Renner, M. W. *Inorg. Chem.* **1986**, *25*, 303.
(15) Tabard, A.; Cocolios, P.; Lagrange, G.; Gerardin, R.; Hubsch, J.; Lecomte, C.; Zarembowitch, J.; Guilard, R. *Inorg. Chem.* **1988**, *27*, 110.
(16) Doppelt, P. *Inorg. Chem.* **1984**, *23*, 4009.
(17) Arasasingham, R. D.; Balch, A. L.; Latos-Grażyński, L. *J. Am. Chem. Soc.* **1987**, *109*, 5846.
(18) Arasasingham, R. D.; Balch, A. L.; Latos-Grażyński, L. In *The Role of Oxygen in Chemistry and Biochemistry*; Ando, W., Moro-oka, Y., Eds. Elsevier: Amsterdam, The Netherlands, 1987; p 417.
(19) Arasasingham, R. D.; Balch, A. L.; Cornman, C. R.; Latos-Grażyński, L. *J. Am. Chem. Soc.* **1989**, *111*, 4357.
(20) Goff, H. M.; Shimomura, E. T.; Lee, Y. J.; Scheidt, W. R. *Inorg. Chem.* **1984**, *23*, 315.
(21) Heistand, R. H., II; Lauffer, R. B.; Fikrig, E.; Que, L., Jr. *J. Am. Chem. Soc.* **1982**, *104*, 2789.
(22) Pyrz, J. W.; Roe, A. L.; Stern, L. J.; Que, L., Jr. *J. Am. Chem. Soc.* **1985**, *107*, 614.
(23) Arasasingham, R. D.; Balch, A. L.; Cornman, C. R.; de Ropp, J. S.; Eguchi, K.; La Mar, G. N. *Inorg. Chem.* In press.

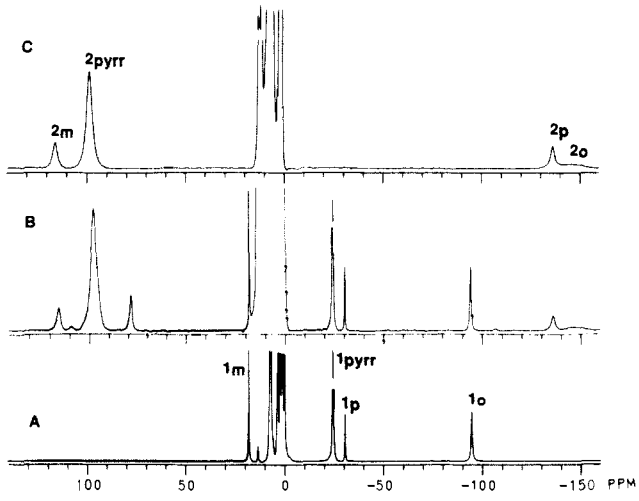

Figure 2. 360-MHz ^{1}H-NMR spectra of toluene-d_8 solutions at −30 °C: (A) TTPFe^{III}(C_6H_5), (B) TTPFe^{III}(C_6H_5) after treatment with dioxygen, and (C) TTPFe^{III}(OC_6H_5). Resonances due to TTPFe^{III}(C_6H_5) are labeled 1, TTPFe^{III}(OC_6H_5), 2. Subscripts identify individual functional groups as in Figure 1 with p, *p*-phenyl, or phenoxy proton. In traces A and B the 1 pyrr resonances have been truncated to fit the available space.

grow into the spectrum that are indicative of the formation of a high-spin iron(III) complex. Comparison of the data with that in Table I allows the resonances to be identified with TTPFe^{III}($OC_6H_4CH_3$-*p*), and trace C of Figure 1 shows the spectrum of an authentic sample of this complex. After oxygenation, some TTPFe^{III}OFe^{III}TTP is also present. The molar ratio of phenoxy-to-μ-oxo product is 3.5:1. These data clearly establish that aryloxy species can be obtained from aryl–iron(III) complexes and that the *p*-tolyl species is converted into the *p*-phenoxy ligand without forming detectable amounts of the meta or ortho forms. This observation indicates a new pathway for oxidation by molecular oxygen that is different from the one seen by Ogoshi and co-workers.[11]

In an attempt to search for possible intermediates, the oxygenations of these aryl–porphyrin complexes were examined at lower temperatures. Oxygenations conducted at −30 °C produce interesting variations. Below that they occur very slowly and were not examined thoroughly. The oxygenation of TTPFe^{III}(C_6H_5) has been examined at both 25 and −30 °C. At 25 °C TTPFe^{III}(OC_6H_5) is the only aryloxy species. However, the results at −30 °C indicate that other products are formed as well. Figure 2 shows the relevant data. Trace A shows the spectrum of TTPFe$^{III}C_6H_5$, trace B shows that sample after the addition of dioxygen, and trace C shows the spectrum of TTPFe^{III}(OC_6H_5). Comparison of traces B and C indicates that TTPFe^{III}(OC_6H_5) is indeed formed. However, additional resonances are present that indicate that other stable species are formed. On warming the sample, these resonances persist. Thus, they represent additional products in the reaction, not intermediates. These products are identified as complexes of hydroquinone.

Trace A of Figure 3 shows the ^{1}H NMR spectrum of TTPFe^{III}(1,4-OC_6H_4O)Fe^{III}TTP in toluene-d_8 at −30 °C generated through the reaction of TTPFe^{II} with *p*-benzoquinone.[24] The resonance assignments shown in the figure have been confirmed through a thorough study which examines the spectroscopic behavior of these binuclear complexes in solution.[25] The pyrrole resonance at 78.3 ppm corresponds to the resonance seen in Figure 2 for the oxygenation of TTPFe^{III}(C_6H_5). The resonance of the bridging hydroquinone ligand at −40 ppm is too broad and too weak to be observed under the conditions necessary to record the spectrum resulting from the dioxygen/TTPFe^{III}(C_6H_5) reaction (trace B, Figure 2). TTPFe^{III}(O-C_6H_4OH-*p*) is also present in the sample. It is formed when TTPFe^{III}OFe^{III}TTP is treated with hydroquinone or when TTPFe^{III}(1,4-OC_6H_4O)Fe^{III}TTP is exposed

(24) Kessel, S. L.; Hendrickson, D. N. *Inorg. Chem.* **1980**, *19*, 1883.

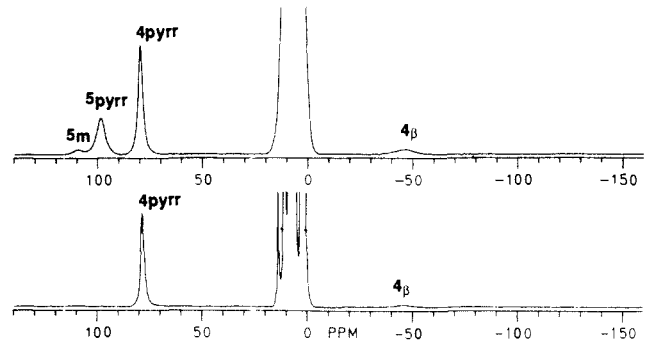

Figure 3. 300-MHz ^{1}H-NMR spectra in toluene-d_8 at −30 °C: (A) TTPFe^{III}(1,4-OC_6H_4O)Fe^{III}(TTP), 4, formed from the reaction of TTPFe^{II} and benzoquinone, (B) a mixture of TTPFe^{III}(1,4-OC_6H_4O)-Fe^{III}(TTP) and TTPFe^{III}(OC_6H_4OH-*p*), 5, formed in the reaction of TTPFe^{III}OFe^{III}TTP with *p*-hydroquinone. Subscripts follow Figure 1 with β referring to the protons of the bridging 1,4-$O_2C_6H_4$ group.

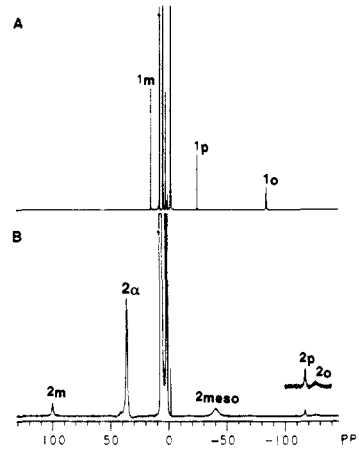

Figure 4. 360-MHz ^{1}H-NMR spectra of toluene-d_8 solutions at 5 °C: (A) OEPFe^{III}(C_6H_5) and (B) OEPFe^{III}(C_6H_5) after the addition of dioxygen for 5 h at 5 °C. Resonances due to OEPFe^{III}(C_6H_5) are labeled 1 and OEPFe^{III}(OC_6H_5), 2. Subscripts identify individual functional groups as in Figures 1 and 2 with α, methylene protons of OEP; meso, meso protons of OEP.

to water.[25] Trace B of Figure 3 shows the ^{1}H NMR spectrum obtained by treating TTPFe^{III}OFe^{III}TTP with hydroquinone; resonances of both TTPFe^{III}(1,4-OC_6H_4O)Fe^{III}TTP and TTPFe^{III}(1,4-OC_6H_4OH) are present. Comparison of the data in trace B of Figure 2 with that of trace B of Figure 3 and the data in Table I allows the resonance at 109 ppm and the added intensity in the composite pyrrole resonance at ca. 95 ppm in trace B (Figure 2) to be identified with the presence of TTPFe^{III}(1,4-OC_6H_4OH).

For comparison with the results of Ogoshi,[11] we monitored the reaction of dioxygen with OEPFe^{III}(C_6H_5) in toluene-d_8 at the lower temperatures characteristic of our conditions. The ^{1}H NMR spectrum of a solution of this complex shows no sign of oxidation at a reasonable rate for our studies below 0 °C. The effects of introducing dioxygen at that temperature are shown in Figure 4. Trace A shows the spectrum of the sample before the addition of dioxygen, while trace B shows the same sample after the addition. As can be seen from the figure, the sample is clearly converted into OEPFe^{III}(OC_6H_5).

The oxygenation in toluene has also been monitored by electron spin resonance spectroscopy. Trace A of Figure 5 shows the ESR spectrum of TTPFe(C_6H_5) in toluene at 9 K. The spectrum is of the strong g_{max} (or HALS, highly anisotropic low spin) variety[26-28] with the intense feature at $g = 3.54$. On warming above

(25) Balch, A. L.; Hart, R. L.; Latos-Grażyński, L. *Inorg. Chem.* In press.
(26) Walker, F. A.; Huynh, B. H.; Scheidt, W. R.; Osvath, S. R. *J. Am. Chem. Soc.* **1986**, *108*, 5288.
(27) Salerno, J. C. *J. Biol. Chem.* **1984**, *259*, 2331.
(28) de Vries, S.; Albracht, S. P. J. *Biochim. Biophys. Acta* **1979**, *546*, 334.

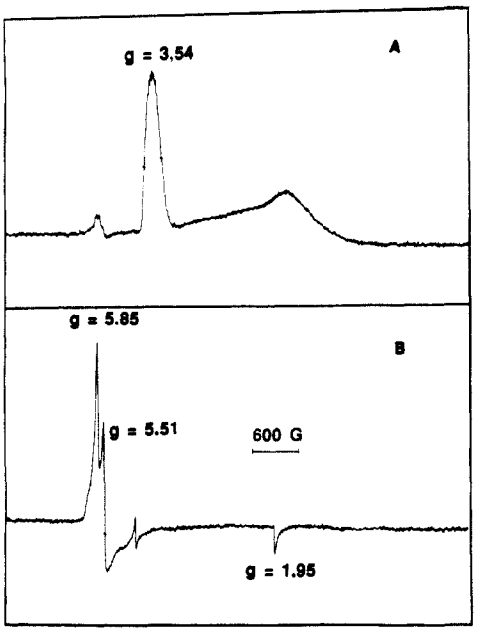

Figure 5. Electron spin resonance spectra of $TTPFe^{III}(C_6H_5)$ in toluene glass at 9 K: (A) A sample whose identity was verified by ^{1}H-NMR spectroscopy. A small amount of a high-spin iron(III) impurity (probably from adventitious dioxygen and a free radical impurity) is present. (B) The sample after warming to 25 °C, adding excess dioxygen, and recooling to 9 K.

30 K, the spectrum disappears as is typical of such strong g_{max} spectra. This appears to be the first model compound with five-coordinate geometry that has been found to give a strong g_{max} spectrum. The lack of near-axial symmetry of this species requires revision of the structural implications that can be drawn from observing a strong g_{max} spectrum.[26] After addition of small quantities of dioxygen at 25 °C and recooling, the spectrum shows the growth of new resonances characteristic of high-spin iron(III) porphyrins and the loss of intensity of the resonances due to the phenyl complex. Trace B of Figure 5 shows the spectrum of the sample after oxygenation is complete, and only the high-spin phenoxy complex is present. The effect of pyridine on the spectrum of $TTPFe^{III}(C_6H_5)$ has also been examined. At 9 K, the spectrum is also of the strong g_{max} type, but it is clearly shifted so that the strong feature has moved to $g = 3.86$ and sharpened somewhat, while the broad feature has moved to higher field. The spectra we report for $TTPFe^{III}(C_6H_5)$ differ from those reported earlier at 115 K.[15] The strong g_{max} signal would not be seen at that temperature. We have not observed the typical low-spin spectrum (g = 1.81, 2.31, 2.63) reported earlier, the high-spin spectrum (g = 6.08, 1,96) described in that report could be the product of inadvertent introduction of dioxygen.

Reaction of $TTPFe^{III}(C_6H_5)$ with Di-*tert*-butyl Peroxide. In order to determine the feasibility of radical displacement as a possible mechanism of formation of phenolate products, we examined the reaction of $TTPFe^{III}(C_6H_5)$ with di-*tert*-butyl peroxide. Figure 6 shows the ^{1}H NMR spectrum of a sample of $TTPFe^{III}(C_6H_5)$ in toluene-d_8 after warming to 100 °C for 12 h. At this temperature di-*tert*-butyl peroxide dissociates into *tert*-butoxy radicals.[29] The product of the $TTPFe^{III}(C_6H_5)$/*tert*-butoxy radical reaction is $TTPFe^{III}O(Bu\text{-}t)$, whose ^{1}H NMR spectrum has been previously described.[30] At lower temperatures the reaction, if any, is much slower. In the absence of dioxygen or di-*tert*-butyl peroxide, $TTPFe^{III}(C_6H_5)$ is stable. A sample of $TTPFe^{III}(C_6H_5)$ withstood heating to 100 °C for 12 h without decompostion.

Reaction of $TTPFe^{III}(C_6H_5)$ with $PFe^{IV}{=}O$. An attempt was made to determine whether we could detect a direct reaction between $TTPFe^{III}(C_6H_5)$ and a ferryl-containing intermediate,

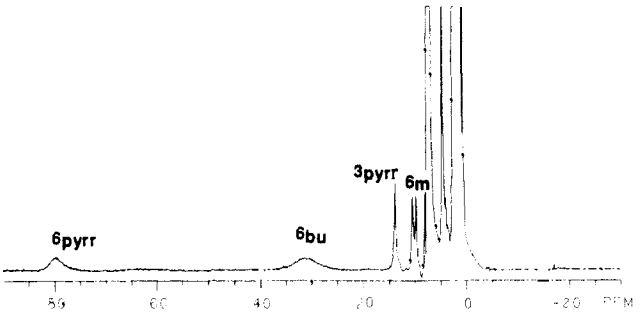

Figure 6. 300-MHz ^{1}H-NMR spectrum at 25 °C of a sample of $TTPFe^{III}(C_6H_5)$ and di-*tert*-butyl peroxide after heating to 100 °C for 12 h. Resonances of $TTPFe^{III}OBu\text{-}t$ are denoted as 6 with subscripts following Figure 1 and bu representing the protons of the *tert*-butoxyl group.

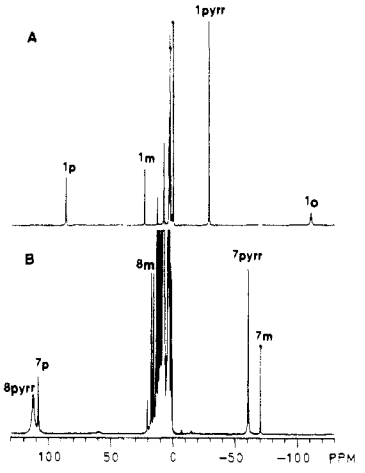

Figure 7. 360-MHz ^{1}H-NMR spectra of chloroform-*d* solutions at −60 °C. (A) $TTPFe^{III}(C_6H_4CH_3\text{-}p)$ and (B) $TTPFe^{III}(C_6H_4CH_3\text{-}p)$ after the addition of dioxygen. Resonances due to $TTPFe^{III}(C_6H_4CH_3\text{-}p)$ are labeled 1, $TTPFe^{IV}(C_6H_4CH_3\text{-}p)^+$, 7, and $TTPFe^{III}Cl$, 8. Subscripts follow the conventions specified in Figure 1.

$TMPFe^{IV}O$.[31] A sample containing a 2:1 molar mixture of $TTPFe^{III}(C_6H_5)$ and $TMPFe^{II}$ was exposed to dioxygen at −78 °C, and the excess dioxygen was removed by 3 freeze–pump–thaw cycles while keeping the sample cooled below −78 °C. The sample was warmed to −30 °C and then to 0 °C. Immediately after warming to −30 °C, it consisted of $TTPFe^{III}(C_6H_5)$ and $TMPFe^{III}OOFe^{III}TMP$. The latter is known to fragment to give $TMPFe^{IV}{=}O$ on standing at −30 °C or on warming above −30 °C.[31] After warming to 0 °C, the sample was reexamined. The peroxo dimer, $TMPFe^{III}OOFe^{III}TMP$, was no longer present, but the resonances characteristic of $TMPFe^{III}OH$ were observed.[31,32] Thus homolysis of the peroxy dimer had occurred. However, resonances of $TTPFe^{III}(C_6H_5)$ remained, and there was no indication of the formation of $TTPFe^{III}(OC_6H_5)$.

Oxygenation of Aryl–Iron(III) Complexes in Chloroform Solution. Different results are obtained when dioxygen is added to $TTPFe^{III}(Ar)$ in chloroform rather than toluene. Representative data are shown in Figure 7. Trace A shows the ^{1}H NMR spectrum of a chloroform solution of $TTPFe^{III}(C_6H_4CH_3\text{-}p)$ at −60 °C in the absence of dioxygen. Upon introduction of dioxygen the spectrum of the sample is converted into that shown in trace B. The resonances of $TTPFe^{III}(C_6H_4CH_3\text{-}p)$ have been replaced with the resonances due to $TTPFe^{III}Cl$ and $[TTPFe^{IV}(C_6H_4CH_3\text{-}p)]^+$. The resonances of the latter are readily identified by comparison with previous work.[10] The resonances characteristic of $TTPFe^{III}(OC_6H_4CH_3\text{-}p)$ are absent from the spectrum. As expected from previous work, $[TTPFe^{IV}(C_6H_4CH_3\text{-}p)]^+$ is not

(29) Benson, S. W.; Shaw, R. In *Organic Peroxides*; Swern, D., Ed.; Wiley-Interscience: New York, 1970; Vol. 1, p 105.
(30) Arafa, I. M.; Goff, H. M.; David, S. S.; Murch, B. P.; Que, L., Jr. *Inorg. Chem.* **1987**, *26*, 2779.
(31) Balch, A. L.; Chan, Y. W.; Cheng, R. J.; La Mar, G. N.; Latos-Grażyński, L.; Renner, M. W. *J. Am. Chem. Soc.* **1984**, *106*, 7779.
(32) Cheng, R. J.; Latos-Grażyński, L.; Balch, A. L. *Inorg. Chem.* **1982**, *21*, 2412.

Table II. ^{1}H NMR Data for Some Iron(IV) Complexes Obtained by Dioxygen Addition

	chemical shifts,[a] ppm						
	Fe–(Ar)				porphyrin aryl		
compound	ortho	meta	para	pyrr	ortho	meta	para
$[TPPFe^{IV}(C_6H_4CH_3\text{-}p)]^+$	b	−71	110	−61	11.4, 10.9	9.2	8.4
$[TTPFe^{IV}(C_6H_4CH_3\text{-}p)]^+$	b	−71	108	−61	11.3, 10.7	9.2	2.4
$[TMPFe^{IV}(C_6H_4CH_3\text{-}p)]^+$	b	−71	108	−61	2.8	11.2, 10.6	2.3
$[TPPFe^{IV}(C_6H_4CH_3\text{-}m)]^+$	b	−104 (−48)[c]	−129	−72	d	d	d

[a] In chloroform-*d* at −60 °C. [b] Not observed in ^{1}H spectrum due to width and large hyperfine shift. [c] Methyl resonance. [d] Not measured.

stable to increasing the temperature. Upon warming to room temperature, all of the resonances of this Fe(IV) species are lost, while the resonances of $TTPFe^{III}Cl$ and $TTPFe^{III}OFe^{III}TTP$ remain and new resonances due to $[TTP(N\text{-}p\text{-}CH_3C_6H_4)Fe^{II}]^+$ develop.

Related Fe(IV)–aryl complexes have been detected upon addition of dioxygen to chloroform solutions of $TPPFe^{III}(C_6H_4CH_3\text{-}p)$, $TMPFe^{III}(C_6H_4CH_3\text{-}p)$, and $TPPFe^{III}(C_6H_4CH_3\text{-}m)$. Relevant chemical shift data for these are compiled in Table II. The slight chemical shift differences reported here for $TPPFe^{IV}(C_6H_4CH_3\text{-}p)^+$ and for $TPPFe^{IV}(C_6H_4CH_3\text{-}p)Br$ in ref 10 reflect the differences in axial ligand as expected. It is not clear in the present work what species, if any, is serving as an axial ligand for the Fe(IV) species when dioxygen is the oxidant.

Discussion

The multiplicity of products seen in the reactions of $PFe^{III}(Ar)$ with dioxygen indicates that there are several pathways that the reaction can take.

The formation of $[TTPFe^{IV}(Ar)]^+$ requires a one-electron oxidation. In the case where dioxygen is the oxidant, the formation of superoxide ion (eq 4) is implied. It is unlikely that the

$$TTPFe^{III}(Ar) + O_2 \rightleftharpoons [TTPFe^{IV}(Ar)]^+ + O_2^- \quad (4)$$

paramagnetic superoxide ion acts as an axial ligand toward the Fe^{IV} product in the experiments reported here. The ^{1}H NMR resonances observed in Figure 7 correspond well to those seen for related complexes with diamagnetic axial ligands. Reaction 4 then implies charge separation and will be favored by a polar solvent environment. Toluene is clearly insufficiently polar to support this reaction. Chloroform and dichloromethane, however, must be sufficiently polar since $[TTPFe^{IV}(Ar)]^+$ does form in them. Moreover, superoxide ion is known to be reactive toward halocarbons.[33] The destruction of superoxide through reaction with these chlorinated solvents is an additional driving force that facilitates the formation of the $[TTPFe^{IV}(Ar)]^+$ product. Degradation of solvent by superoxide also provides a source of chloride ion that is found in the other product ($TTPFe^{III}Cl$) of oxygenation of $TTPFe^{III}(Ar)$ in chlorocarbon solvents.

In toluene a different pattern of reaction occurs that results in the formation of aryloxy complexes. One likely course of the reaction is initial insertion of dioxygen into the Fe–C bond (eq 5) followed by rapid homolysis of the transient aryl peroxide complex (eq 6). In this case homolysis of the aryl peroxide

$$PFe^{III}(Ar) + O_2 \rightarrow PFe^{III}OOAr \quad (5)$$

$$PFe^{III}OOAr \rightarrow PFe^{IV}O + {}^{\bullet}OAr \quad (6)$$

complex is expected on the basis of our early observations of homolysis of $Fe^{III}OOBu\text{-}t$ units,[34,35] the low polarity of the solvent, and the resonance stabilization of the aryloxy radical. Reaction 5 corresponds to the behavior already documented for Fe^{III}–alkyl complexes in toluene where the alkyl peroxide intermediates can be directly observed by NMR spectroscopy.[17-19] In the present case, however, an aryl peroxide would be expected to be exceedingly short-lived. Note that the hypothetical aryl hydroperoxides and diaryl peroxides are unknown substances.[36]

The formation of the phenoxy products then can be accounted for by two subsequent reactions (eqs 7 and 8). There is precedent

$$PFe^{III}(Ar) + {}^{\bullet}OAr \rightarrow PFe^{III}(OAr) + {}^{\bullet}Ar \quad (7)$$

$$PFe^{IV}{=}O + {}^{\bullet}Ar \rightarrow PFe^{III}(OAr) \quad (8)$$

for the radical displacement reaction (eq 7). *tert*-Butoxy radicals (generated by thermolysis of di-*tert*-butyl peroxide) react with $TTPFe^{III}(C_6H_5)$ to form $TTPFe^{III}(O\text{-}Bu\text{-}t)$ cleanly (Figure 6). Alternately the reaction may occur through the sequence of eqs 9 and 10. However, reaction 9 does not appear to be particularly

$$PFe^{IV}{=}O + PFe^{III}(Ar) \rightarrow PFe^{III}(OAr) + PFe^{II} \quad (9)$$

$$PFe^{II} + {}^{\bullet}OAr \rightarrow PFe^{III}(OAr) \quad (10)$$

appealing since it requires the transfer of a phenyl group from one iron to a ferryl group and the close approach of two porphyrin complexes. Reaction 7, which can be accomplished by the backside attack of the phenoxy radical on $TTPFe^{III}(Ar)$, is much more appealing and, of course, has precedent. We attempted to model reaction 9 by examining a mixture in which $TTPFe^{III}(C_6H_5)$ and $TMPFe^{IV}O$ (generated by homolysis of $TMPFe^{III}OOFe^{III}TMP$)[31] were both present. No evidence was found for the formation of $TTPFe^{III}(OC_6H_5)$ in this reaction. While this experiment may be criticized because of the bulky nature of $TMPFe^{IV}{=}O$ relative to the other porphyrins involved, it does present an example where a known, observed ferryl complex[31] can be generated in the presence of an iron–aryl complex. In this case no reaction was detected.

The formation of aryloxy complexes upon oxygenation cannot result from simple homolysis of an Fe–C bond followed by reaction of the resulting aryl radical with dioxygen. It is well-known that phenyl radicals are unreactive toward dioxygen and that they couple to form biphenyl even in the presence of dioxygen.[37,38] There is a fundamental difference in our oxygenation experiments run at or below 25 °C which produce aryl oxide ligands and those of Ogoshi et al. run at 80 °C which produce biphenyl. In the latter experiment, it is likely that thermal homolysis of $OEPFe^{III}Ph$ occurs. This is followed both by coupling of the product phenyl radicals and by the reaction of $OEPFe^{II}$ with dioxygen to form $OEPFe^{III}OFe^{III}OEP$.

The formation of complexes derived from *p*-hydroquinone requires comment. A plausible path for this reaction involves attack of the ferryl complex on a phenoxy radical (eq 11). Formation of the dimeric complex, $PFe^{III}(1,4\text{-}OC_6H_4O)Fe^{III}P$, may then result from the dehydration step shown in eq 12. The yield of products obtained via reactions 11 and 12 increases when the oxygenation is performed at −30 °C rather than at 25 °C. This is readily explained if one assumes that reaction 11 occurs within a cage after the homolysis of the aryl hydroperoxide (eq 6). By lowering the temperature, escape from the cage is slowed, and the effects of eq 11 may be detected. The reaction of Frémy's salt with phenols is known to produce quinones via the mechanism shown in eq 13.[39-41] This forms a very close parallel to what is

(33) Roberts, J. L., Jr.; Sawyer, D. T. *J. Am. Chem. Soc.* **1981**, *103*, 712.
(34) Arasasingham, R. D.; Cornman, C. R.; Balch, A. L. *J. Am. Chem. Soc.* **1989**, *111*, 7800.
(35) Balch, A. L.; Hart, R. L.; Latos-Grażyński, L.; Traylor, T. G. *J. Am. Chem. Soc.* In press.
(36) (a) Hock, H.; Ernst, F. *Chem. Ber.* **1959**, *92*, 2732. (b) *Organic Peroxides*; Swern, D., Ed.; Wiley-Interscience: New York, 1970; vol. 1, 1971; Vol. 2, 1972; Vol. 3.
(37) Russell, G. A.; Bridger, R. F. *J. Am. Chem. Soc.* **1963**, *85*, 3765.
(38) Garst, J. F.; Smith, C. D.; Farrar, A. C. *J. Am. Chem. Soc.* **1972**, *94*, 7707.

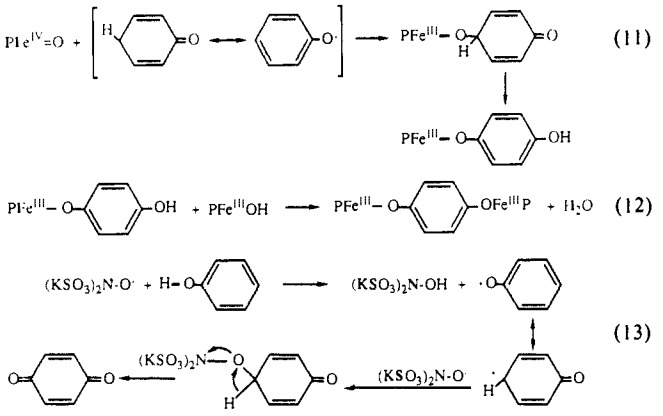

proposed in reaction 11. In related work, Seok and Meyer[42] have shown that complexes containing the Ru^{IV}=O group are capable of oxidizing phenols to quinones. It is unlikely that the *p*-hydroquinone derived complexes arise from the reaction of the phenoxy radical with dioxygen. It is known that the reactivity of phenoxy radicals, like phenyl radicals, toward dioxygen is low[37] and that radical/radical coupling is favored over reaction with dioxygen.[43]

Peroxidases are known to catalyze oxidations of phenols,[44-46] However, our current picture of the heme cavity in the horseradish peroxidase seems to preclude, in most cases, direct interaction of ferryl states with substrates whose entry to the heme pocket is restricted.[47] Thus, these enzymatic oxidations are likely to involve reactions fundamentally different than those studied here where the phenoxy radical is generated in the immediate vicinity of the iron porphyrin.

Experimental Section

Materials. Samples of $TTPFe^{III}(Ar)$ were prepared from $TTPFe^{III}Cl$ and the appropriate Grignard reagent by an established procedure[11-13] and handled in a dioxygen-free glovebox. Samples of $TTPFe^{III}(OAr)$ were prepared by addition of an excess of the solid sodium salt of the phenolate to $TTPFe^{III}Cl$ in toluene or chloroform solution, sonication of the mixture, and filtration to remove the sodium phenolate and sodium chloride. Toluene-d_8, chloroform-*d*, and dichloromethane-d_2 were deoxygenated and stored in a dinitrogen-filled glovebox before use.

Oxygenation Experiments. A 3 mM solution of $TTPFe^{III}(Ar)$ in toluene-d_8, chloroform-*d*, or dichloromethane-d_2 was prepared under a dinitrogen atmosphere, placed in a 5-mm NMR tube, sealed with a rubber septum cap, and wrapped with Parafilm. Dioxygen was admitted to the sample through a microliter syringe while controlling the temperature of the sample. The sample was shaken to facilitate dioxygen uptake and placed in the NMR spectrometer for spectral observation.

Instrumentation. NMR spectra were recorded on Nicolet NT-360 FT and NT-500 FT spectrometers operating in the quadrature mode (^1H frequencies are 360 and 500 MHz, respectively). The spectra were collected over a 40-kHz bandwidth with 16 K data points and a 6-μs 90° pulse. For a typical paramagnetic spectrum, between 500 and 2000 transients were accumulated with a delay time of 50 ms. The signal-to-noise ratio was improved by apodization of the free induction decay. The residual methyl peak of toluene was used as a secondary reference, which was set at 2.09 ppm. To obtain line widths of overlapping resonances, the spectra were deconvoluted by using the NTC CAP routine of the Nicolet software. ESR spectra were recorded on a Bruker spectrometer at X band.

Acknowledgment. We thank the National Institutes of Health (Grant GM-26226) for support.

(39) Waters, W. A. *Mechanisms of Oxidation of Organic Compounds*; Methnen and Co.: London, 1964; p 147.
(40) Teuber, H. J.; Dietz, K. H. *Angew. Chem., Int. Ed. Engl.* **1965**, *4*, 871.
(41) Zimmer, H.; Lankin, D. C.; Horgan, S. W. *Chem. Rev.* **1971**, *71*, 229.
(42) Seok, W. K.; Meyer, T. J, *J. Am. Chem. Soc.* **1988**, *110*, 7358.
(43) Blanchard, H. S. *J. Org. Chem.* **1960**, *25*, 264.
(44) Hewson, W. D.; Dunford, H. B. *J. Biol. Chem.* **1976**, *251*, 6043.
(45) Shiga, T.; Imaizumi, K. *Arch. Biochem. Biophys.* **1975**, *167*, 469.
(46) Buhler, D. R.; Mason, H. S. *Arch. Biochem. Biophys.* **1961**, *92*, 424.
(47) Ortiz de Montellano, P. R. *Acc. Chem. Res.* **1987**, *20*, 289.

Production and Storage of Multiple, Photochemical Redox Equivalents on a Soluble Polymer

Laura A. Worl,[1a] Geoffrey F. Strouse, Janet N. Younathan,[1b] Steven M. Baxter, and Thomas J. Meyer*

Contribution from the Department of Chemistry, University of North Carolina, Chapel Hill, North Carolina 27599. *Received December 18, 1989*

Abstract: Soluble polymers have been prepared that contain high loadings of metal-to-ligand charge-transfer (MLCT) visible-light absorbers based on polypyridyl complexes of Ru^{II} or Os^{II}. The complexes have been attached to a styrene/chloromethylstyrene copolymer by nucleophilic displacement of the chloro groups. By using excesses of the complexes, complete substitution at the available ~30 chloro-methylated sites was achieved. A series of mixed-valence polymers with controlled M^{III}/M^{II} ratios has been prepared in acetonitrile or acidic aqueous solution by oxidation with Ce(IV). For the Os^{II}-containing polymers, Os^{II*}-based MLCT excited-state lifetimes and emission quantum yields are relatively unaffected by the Os^{III}/Os^{II} ratio. This shows that intramolecular oxidative quenching of Os^{II*} by Os^{III} is slow. The slow rate of electron-transfer quenching is a manifestation of the "inverted region". Because excited-state properties are relatively unaffected in the mixed-valence polymers, it is possible to build up and store ~30 oxidative equivalents on individual polymeric strands by photochemical oxidation.

Introduction

In molecular systems, well-defined processes exist in which single photon excitation leads to the production of redox equivalents with relatively high efficiency,[2,3] e.g., eq 1 where PQ^{2+} =

$$Ru(bpy)_3^{2+} \xrightarrow{h\nu} Ru(bpy)_3^{2+*} \quad (1a)$$

$$Ru(bpy)_3^{2+*} + PTZ \rightarrow Ru(bpy)_3^{+} + PTZ^{+} \quad (1b)$$

$$Ru(bpy)_3^{2+*} + PQ^{2+} \rightarrow Ru(bpy)_3^{3+} + PQ^{+} \quad (1c)$$

(1) (a) Current address: Los Alamos National Labs, Los Alamos, NM 87545. (b) Current address: Eastman Kodak Company, Rochester, NY 14650.

0002-7863/90/1512-7571$02.50/0 © 1990 American Chemical Society